Acta Cryst. (1975). A31, 126

Antiphase Domains in a Lunar Pigeonite: Determination of the Average Shape, Size and Orientation from a Measurement of Three-Dimensional Intensity Profiles of Diffuse ($h+k=$odd) Reflections

BY MARTHA M. HAMIL

Department of Geology, Rutgers University, New Brunswick, New Jersey, 08903, *U.S.A.*

AND SUBRATA GHOSE

Department of Geological Sciences, University of Washington, Seattle, Washington 98195, *U.S.A.*

AND ROBERT A. SPARKS

Syntex Analytical Instruments, Cupertino, California, U.S.A.

(*Received* 19 *May* 1973; *accepted* 14 *August* 1974)

Three-dimensional intensity profiles of selected diffuse *b*-type ($h+k=$odd) reflections in a core pigeonite from lunar rock 12053 have been measured by a point-count method using a single-crystal automatic diffractometer. Sampling reciprocal space about a Bragg reflection yields a $5\times5\times5$ array of intensity data; contouring shows the shape, size and orientation of the diffuse reflection. It is assumed that the intensity distribution is Gaussian in reciprocal space and the diffuseness of the *b*-type reflections is primarily due to small antiphase domains. From the intensity data, the average shape, size and orientation of the antiphase domains have been determined by applying Fourier transform theory. The average shape of the antiphase domains can be approximated by an ellipsoid with axial lengths; $\bar{z}=171$, $\bar{y}=141$, and $\bar{x}=122$ Å. Lengths of these axes have been adjusted by a correction factor which makes the adjacent *a*-type ($h+k=$even) reflection conform to its ideal spherical form. The long (z) axis deviates from the crystallographic axis and forms a 44° circle about $\bar{2}11$. The average size and shape of the domains agree well with those determined through electron microscopy.

Introduction

Crystals showing simultaneously sharp and diffuse X-ray reflections due to mistakes in the structure are well known, one such case being crystals with small antiphase domains. The diffuseness is caused by the small domain size and is comparable to the line broadening in powder diffraction due to small particle size. In pigeonite the *b*-type ($h+k=$odd) reflections are sometimes diffuse because of the presence of small antiphase domains. We have measured three-dimensional intensity profiles of the selected *b*-type diffuse reflections in a core pigeonite from lunar rock 12053 by a point-count method using a single-crystal automatic diffractometer. The results of such measurements yield the shape, size and orientation of the diffuse reflections in three-dimensional reciprocal space. Assuming the intensity distribution to be Gaussian in reciprocal space, from these data, we have determined the average shape and size, as well as, orientation of the antiphase domains with respect to the crystallographic axes applying Fourier transform theory. In the present paper, our method has been applied to a lunar pigeonite. We would like to point out, however, that our method is a perfectly general one and can be applied to other crystals, such as plagioclase feldspars, showing diffuse X-ray reflections due to small antiphase domains.

Antiphase domains in pigeonite

Pigeonites are monoclinic pyroxenes within the system $CaSiO_3$–$MgSiO_3$–$FeSiO_3$, the $CaSiO_3$ component varying between 5 and 15 mol. %. At room temperature the space group is $P2_1/c$ (Morimoto, 1956; Bown & Gay, 1957). At high temperatures, pigeonite undergoes a displacive phase transformation, the space group being $C2/c$ (Prewitt, Papike & Ross, 1970). Antiphase domains are generated during the $C2/c$ to $P2_1/c$ phase transformation (Morimoto & Tokonami, 1969). Hence, *b*-type ($h+k=$odd) reflections, which appear during the phase transformation, are closely related to the formation of the antiphase domains. In the $C2/c$ phase, there is only one type of silicate chain, while in the $P2_1/c$ phase, there are two types of crystallographically distinct silicate chains, *A* and *B*, the *B*-chain being more kinked than the *A*-chain (Brown, Prewitt, Papike & Sueno, 1972). When pigeonites are cooled from magmatic temperatures, mistakes in ordering of the chains along **a** and **b** directions in the crystal occur during the $C2/c$ to $P2_1/c$ transformation. These mistakes account for the antiphase boundary. The postulated displacement vector, which brings the antiphase domains into register, is $\mathbf{a}/2+\mathbf{b}/2$ (Morimoto & Tokonami, 1969). The antiphase domains in pigeonite have been directly observed in the electron microscope by imaging through the *b*-type reflections (Bailey *et al.*, 1970; Christie *et al.*,

1971; Champness & Lorimer, 1971; Ghose, Ng & Walter, 1972). Empirically it has been observed that when the size of the antiphase domains is smaller than *ca.* 1000 Å, the *b*-type reflections are diffuse (Ghose *et al.*, 1972). When the antiphase domains are small (below 100 Å), it is difficult to resolve them through the electron microscope and determine the shape and size of the domains directly. Furthermore, getting a three-dimensional view of the domains through electron microscopy is difficult, if not impossible. In such cases, measurement of the three-dimensional profiles of diffuse *b*-type reflections in reciprocal space can yield the average shape, size and orientation of the antiphase domains.

Experimental

We selected a yellow pigeonite fragment, showing very faint diffuse reflections from exsolved augite and diffuse *b*-type reflections in (*h*0*l*) precession photographs (Fig. 1). The crystal data are listed in Table 1. Electron microprobe analysis of the same crystal used for intensity measurements indicated that the crystal is chemically quite homogeneous, with an approximate composition: $(Ca_{0.19}Fe_{0.59}Mg_{1.22})Si_2O_6$.

Table 1. *Crystal data on pigeonite from rock* 12053

Cell dimensions	
a_0	9·686 (3) Å
b_0	8·890 (3)
c_0	5·239 (2)
β	108·5 (4)°
Space group $P2_1/c$	
Size of crystal (mm)	0·10 × 0·13 × 0·24
Linear absorption coefficient, (cm^{-1})	31

Cell dimensions and intensities were measured on a Syntex $P\bar{1}$ automatic single-crystal diffractometer using monochromatic Mo $K\alpha$ radiation and a solid-state detector system. Least-squares refinement with 1003 reflections, using anisotropic temperature factors, yielded an R value of 0·042. The site occupancies are $M2$: Ca 0·18, Fe 0·47 and Mg 0·35, and $M1$: Mg 0·87 and Fe 0·13. The details of the pigeonite crystal structure are comparable to other terrestrial and lunar pigeonite structures refined so far (Morimoto & Güven, 1970; Clark, Ross & Appleman, 1971; Takeda, 1972; Brown *et al.*, 1972).

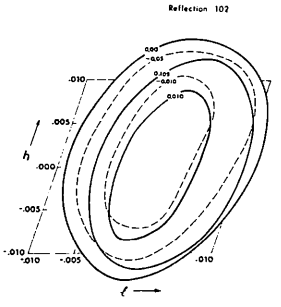

Fig. 2. A three-dimensional view of the diffuse 102 pigeonite reflection in reciprocal space. Contours are at intervals of $I=200$ counts.

The three-dimensional intensity profiles of a number of selected adjacent *a* and *b*-type reflections were measured using a point-count method. The point-count method samples a $5\times5\times5$ grid of reciprocal space about a Bragg reflection by treating h, k, and l as variables.

The sampling grid is a parallelepiped with edges parallel to the reciprocal cell axes. Increments in h, k, and l depend on the length of reciprocal cell axes and are calculated so that the sampling positions provide complete coverage of the diffracting volume. For this 12053 pigeonite $\Delta h=0{\cdot}02490$ $Å^{-1}$. The reciprocal volume sampled at each grid point was $4{\cdot}628\times10^{-5}$ $Å^{-3}$. During recording the detector window is closed down to about $0{\cdot}2\times0{\cdot}2$ mm to eliminate integration of the intensities. Point counts were made for 1·5 min at each grid point. Contours of the $5\times5\times5$ array of intensity data show the size, shape and orientation of a diffuse Bragg reflection in reciprocal space. The $I=200$ count contours for the diffuse 102 reflection are shown in Fig. 2.

The diffracting volume in reciprocal space

In order to obtain the shape and size of the diffracting volume around a Bragg reflection we made the following assumptions:

1. The intensity distribution is Gaussian in reciprocal space.
2. Thermal diffuse scattering does not change the shape of a diffracting volume but may broaden it.
3. Diffracting volume in an ideal crystal is spherical.
4. Observed intensity distribution is intensity distribution of an ideal crystal convoluted by a 'smearing' function.

Assumptions 1 and 4 taken together imply that the 'smearing' function is Gaussian. The intensity at a point in reciprocal space is given by

$$I(\mathbf{s})=I_0pF^*FG(\mathbf{s})\,, \qquad (1)$$

where $\mathbf{s}$ is a continuous variable in reciprocal space, p is the polarization factor, $I_0=I_{\text{beam}}e_4/R^2m^2c^4$, where R is the distance, e and m are charge and mass of an electron, and c is the velocity of light; and $G(\mathbf{s})$ is some distribution function. All quantities on the right-hand side except $G(\mathbf{s})$ are constant in the vicinity of a particular reciprocal-lattice node designated hkl. Equation (1) implies that around each reciprocal-lattice node occurs a distribution of intensities determined by $G(\mathbf{s})$. Therefore, $G(\mathbf{s})$ contains all those factors that affect the size and shape of the diffracting volume such as crystal shape, thermal diffuse scattering, domain structure, and other order–disorder effects. In order for $G(\mathbf{s})$ to

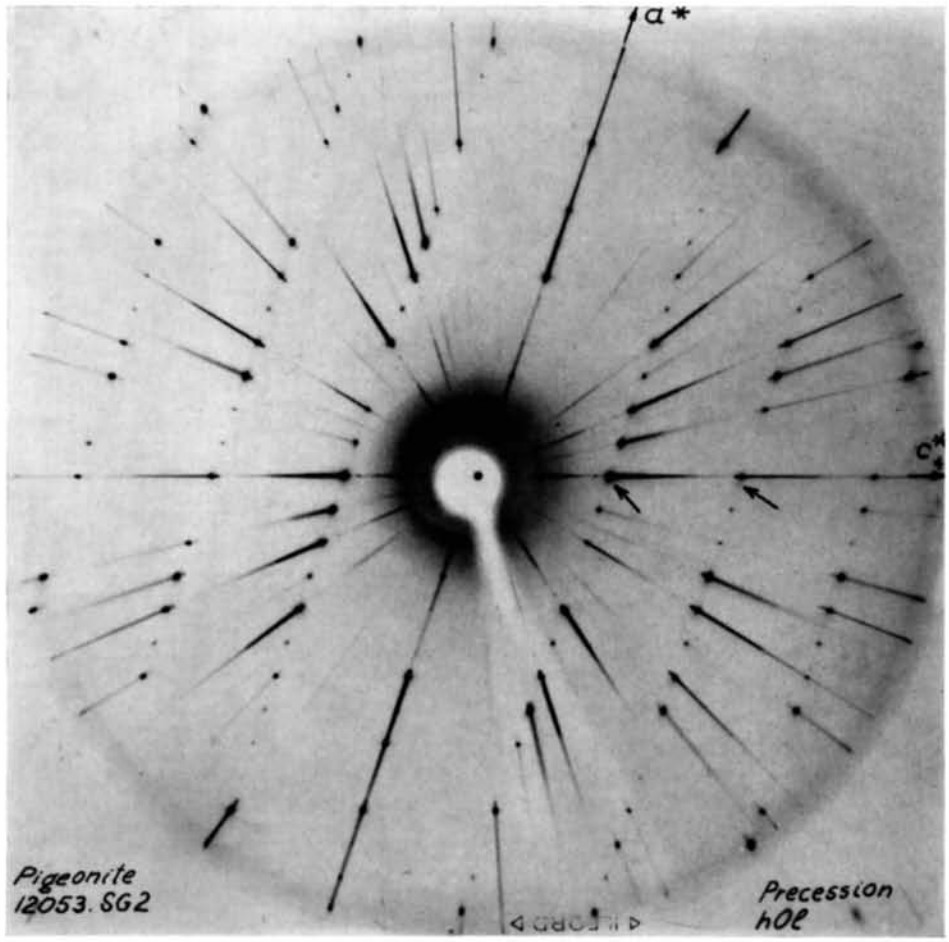

Fig. 1. Precession photograph (*h0l*) of lunar pigeonite from rock 12053. Note *b*-type ($h+k=$ odd) reflections are diffuse and stretched parallel to **a***. Diffuse reflections from very fine exsolved augite lamellae parallel to the (100) plane are indicated by arrows.

[*To face p.* 127

be a distribution function in three dimensions, it must have the form

$$G(\mathbf{s}) = C_N \exp\left(-\tfrac{1}{2}\mathbf{s}^T\mathbf{U}^{-1}\mathbf{s}\right), \quad (2)$$

where C_N is the normalization constant and $\mathbf{U}$ is a symmetric metric tensor. At this point all we know about $\mathbf{U}$ is that it is a conicoid, but *a priori* we expect it to be some real quadric, probably an ellipsoid, whose eigenvalues and eigenvectors give the size, shape, and orientation of the diffracting volume in reciprocal space.

To measure $I(\mathbf{s})$ as a function of position in reciprocal space, we set up a $5\times5\times5$ grid about each Bragg reflection. Because the center of the diffracting volume is not necessarily at the center of the grid we rewrite equation (2) to include the center as

$$G(\mathbf{s}) = C_N \exp\left[-\tfrac{1}{2}(\mathbf{s}-\mathbf{h})^T\mathbf{U}^{-1}(\mathbf{s}-\mathbf{h})\right], \quad (3)$$

where $\mathbf{h}$ represents the coordinates of the center. Equation (1) now becomes

$$I(\mathbf{s}) = I_0 pF^*F \exp\left[-\tfrac{1}{2}(\mathbf{s}-\mathbf{h})^T\mathbf{B}(\mathbf{s}-\mathbf{h})\right], \quad (4)$$

where $\mathbf{B}=\mathbf{U}^{-1}$ and I_0 includes C_N. We now need to find I_0, $\mathbf{h}$, and $\mathbf{B}$. With the natural log of both sides of equation (4) taken to convert it to linear form,

$$-2\log I(\mathbf{s}) = -2\log(I_0F^*Fp) + (\mathbf{s}-\mathbf{h})^T\mathbf{B}(\mathbf{s}-\mathbf{h}). \quad (5)$$

Because this equation contains too many unknowns for least-squares methods to be used, we first determine $\mathbf{h}$ as the centroid of the intensity distribution. Equation (5) is expanded to

$$\begin{aligned}-2\log I(\mathbf{s}) + 2\log(F^*Fp) &= (s_1-h_1)^2b_{11}\\ &+2(s_1-h_1)(s_2-h_2)b_{12}+2(s_1-h_1)(s_3-h_3)b_{13}\\ &+2(s_2-h_2)^2b_{22}+2(s_2-h_2)(s_3-h_3)b_{23}\\ &+(s_3-h_3)^2b_{33}-2\log I_0. \end{aligned} \quad (6)$$

We can apply the method of least squares (Nye, 1957) by letting $\mathbf{A}$ be the column vector of the left-hand side of equation (6), $\boldsymbol{\theta}$ be the 125×7 array of coefficients of b_{ij} and $\log I_0$, and $\boldsymbol{\alpha}$ be the column vector containing the B_{ij}'s and $\log I_0$ so that

$$\boldsymbol{\alpha} = (\boldsymbol{\theta}^T\boldsymbol{\theta})^{-1}\boldsymbol{\theta}^T\mathbf{A}. \quad (7)$$

The first six terms of $\boldsymbol{\alpha}$ form the 3×3 symmetric metric tensor $\mathbf{B}$, whose eigenvalues and eigenvectors may be found by standard methods after converting $\mathbf{B}$ to an orthonormal basis, $\mathbf{B}^0$. The eigenvectors give the principal axes in reciprocal space and the eigenvalues B_1, B_2, B_3 give the principal-axis representation

$$B_1s_1^2 + B_2s_2^2 + B_3s_3^2 \quad (8)$$

to the quadratic form $\mathbf{s}^T\mathbf{B}\mathbf{s}$; $1/\sqrt{B_i}$ is the length of the principal axes. Applying Fourier methods to $G(\mathbf{s})$, its transform in crystal space is

$$W(\mathbf{x}) = \exp\left(-\tfrac{1}{2}\mathbf{x}^T\mathbf{U}\mathbf{x}\right) \quad (9)$$

so that $\mathbf{U}$ is a quadric tensor in crystal space, with eigenvalues U_1, U_2, U_3. As $\mathbf{U}=\mathbf{B}^{-1}$, its eigenvalues are $1/B_i$ (Hohn, 1964) and the eigenvectors are the same as those of B_i, if $\mathbf{B}$ and $\mathbf{U}$ have been converted to an orthonormal basis set.

Determination of the size, shape and orientation of the antiphase domains

The quadric tensor $\mathbf{U}$ represents in crystal space those factors that contribute to the size and shape of the diffracting volume of a lattice node, which include the external shape of the crystal, thermal diffuse scattering and small subgrain boundaries. Therefore, all known contributing factors must be eliminated from $\mathbf{U}$ in order to interpret its physical significance.

Adjacent nodes in the reciprocal lattice should re-

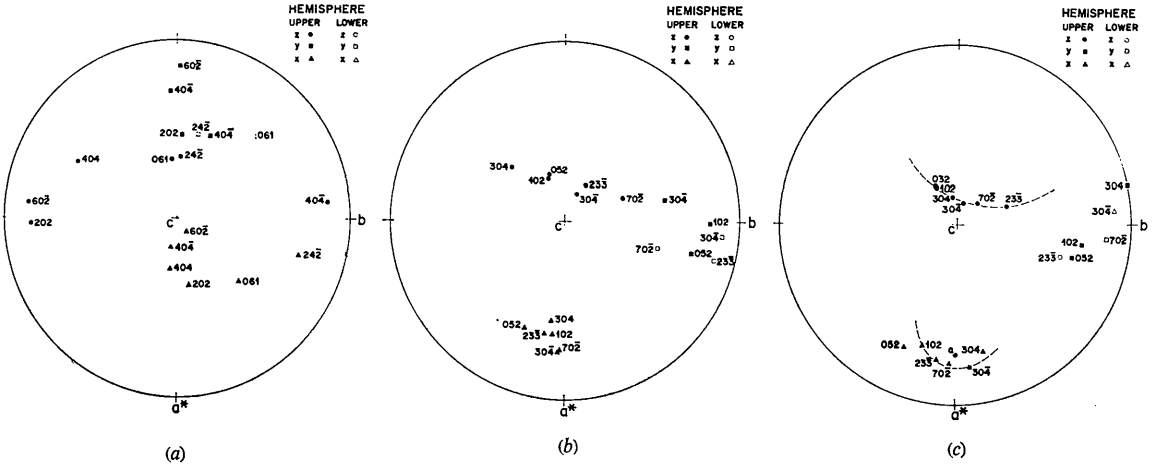

(a) (b) (c)

Fig. 3. Stereographic projection of ellipsoidal axes of (*a*) *a*-type reflections adjacent to (*b*) uncorrected *b*-type reflections, and (*c*) corrected *b*-type reflections.

flect the external form factor similarly, that is, the shape of the diffracting volume of adjacent nodes caused by the external shape of the crystal should be the same. Therefore adjacent *a*- and *b*-type reflections should have the same contribution from the external form factor. Neglecting thermal diffuse scattering and assuming that the shape of the reflecting region is spherical in an ideal crystal and that the *a*-type reflections represent the least deviation from the ideal situation, we can remove the effects that cause any deviation from sphericity of the *a*-type reflections.

Letting **A** represent the tensor of the *a*-type reflections and **S** the ideal spherical form of the *a*-type reflections, then there exists some quadric **E** such that

$$\mathbf{A}-\mathbf{E}=\mathbf{S} \qquad (10)$$

where $A_1A_2A_3=S_1S_2S_3$ and $S_1=S_2=S_3$. That is, **E** converts **A** into a sphere. Subtracting **E** from the tensor of the adjacent *b*-type reflections, **O**, such that

$$\mathbf{O}-\mathbf{E}=\mathbf{T}, \qquad (11)$$

then applies the same correction to **O**. If the *b*-type reflection is spherical the eigenvalues, λ_i, of **T** should all be equal. Otherwise, they represent the deviations from sphericity.

The eigenvectors of **A** [Fig. 3(*a*)] are dispersed on a spiral curve and do not appear random. The eigenvectors of **O** [Fig. 3(*b*)] are less widely distributed. The *X* axis which is the long axis of the reflecting volume in reciprocal space falls very close to the [102] direction whereas the *Z* axis forms a small circle. Finding the tensor **E** for each *a*-type reflection and applying it to **O** yields the distribution of eigenvectors shown in Fig. 3(*c*). The *Z* axes fall on a 44° small circle about $\bar{2}11$. The short axes are spread somewhat about [102]. However, the short and intermediate axes of $30\bar{4}$ are interchanged.

As the *a*-type reflections are elongated they become diffuse but the directions [Fig. 3(*a*)] of elongation are not such that they would be ordinarily observed. This distortion of the *a*-type reflections is caused in part by the shape of the crystal. However, this distortion should have a constant orientation which is overprinted by either a fine-scale mosaic structure or elastically distorted cell parameters or some combination of these two. The above procedure compensates for any such structures present in pigeonite which could cause diffuseness of both *a*- and *b*-type reflections.

The lengths and orientations of the principal axes of the antiphase domains, determined from six strong diffuse reflections, are listed in Table 2. Lengths of these axes have been adjusted using equation (11). It is significant that the orientation of the long axes of the antiphase domains form a small circle [Fig. 3(*c*)]. The cause of this deviation is not clear at present.

Another significant factor present in Table 2 which is unexplained at present is that the lengths of the axes vary among the Bragg reflections, giving an apparent size dependence on *hkl*. This may be attributable to:

1. dependence on *hkl*, or
2. dependence on 2θ, or
3. dependence on *I*, or
4. dependence on *F*.

Dependence on *hkl* and 2θ are similar in that they imply that orientation of the domains with respect to the X-ray beam gives different results or that thermal diffuse scattering is not negligible. A dependence on *I* would indicate that an unknown factor has not been included. The fourth possibility has been eliminated because *F* appears in the calculations.

The apparent size dependence on *hkl* is not a new problem and has been noted by Guinier (1963, p. 270) and Brown *et al.* (1972). Thus it appears to be a basic unexplained observation in antiphase domain studies.

Table 2. *Lengths of principal axes of domains and their orientations*

Reflection	Axis	Axial length (Å)	Orientation (°) *a**	*b*	*c*
	z	181	113	104	27
102	*y*	143	81	21	71
	x	125	153	74	109
	z	270	103	86	14
$30\bar{4}$	*y*	148	166	96	103
	x	136	85	172	84
	z	168	107	93	17
304	*y*	139	103	13	90
	x	129	22	78	73
	z	193	104	77	19
$70\bar{2}$	*y*	136	96	167	78
	x	116	15	93	76
	z	169	113	104	28
052	*y*	146	75	27	68
	x	120	152	68	107
	z	176	100	59	33
$23\bar{3}$	*y*	149	105	148	62
	x	121	18	98	74
	z	171	104	80	17
Mean	*y*	141	129	62	52
	x	122	24	109	75

Discussion

From precession photographs of Mull pigeonite, Morimoto & Tokonami (1969) have observed that the diffuse *b*-type reflections are disc shaped, being stretched parallel to **a*** and **b***. From two-dimensional line profiles of these reflections measured on a diffractometer, they concluded that the antiphase domains are columnar in shape, the long axis being parallel to the crystallographic *c* axis. On the other hand, our analysis indicates that the antiphase domains are ellipsoidal in shape, the long axis deviating considerably from the *c* axis. This observation has also been made by Heuer and his colleagues from the shape and orientation of diffuse *b*-type spots in electron diffraction patterns of lunar pigeonites (A. H. Heuer, 1972, oral communication).

The shape and size of the antiphase domains in this pigeonite are in fair agreement with those observed

through electron microscopy, which shows that the antiphase domains are rounded to blocky in shape, about 50–100 Å in diameter (see Fig. 6 in Ghose, Ng & Walter, 1972).

The measurement of the three-dimensional intensity profiles were carried out at Syntex Analytical Instruments, Cupertino, California. This research has been supported by NASA grant NGR 05-003-486.

References

BAILEY, J. C., CHAMPNESS, P. E., DUNHAM, A. C., ESSON, J., FYFE, W. S., MACKENZIE, W. S., STUMPFL, E. F. & ZUSSMAN, J. (1970). *Proc. Apollo* 11 *Lunar Sci. Conf., Geochim. Cosmochim. Acta, Suppl.* 1, Vol. 1, pp. 169–194.

BOWN, M. G. & GAY, P. (1957). *Acta Cryst.* **10**, 440–441.

BROWN, G. E., PREWITT, C. T., PAPIKE, J. J. & SUENO, S. (1972). *J. Geophys. Res.* **77**, 5778–5789.

CHAMPNESS, P. E. & LORIMER, G. W. (1971). *Contrib. Miner. Petrol.* **33**, 171–183.

CHRISTIE, J. M., LALLY, J. S., HEUER, A. H., FISHER, R. M., GRIGGS, D. T. & RADCLIFFE, S. V. (1971). *Proc. 2nd Lunar Sci. Conf.*, Vol. 1, pp. 68–89. Boston: M.I.T. Press.

CLARK, J., ROSS, M.& APPLEMAN, D. (1971). *Amer. Min.* **56**, 888–908.

GHOSE, S., NG, G. & WALTER, L. S. (1972). *Proc. 3rd Lunar Sci. Conf. Geochim. Cosmochim. Acta, Suppl.* 3, Vol. 1, pp. 507–531.

GUINIER, A. (1963). *X-Ray Diffraction.* San Francisco: W. H. Freeman.

HOHN, F. E. (1964). *Elementary Matrix Algebra*, 2nd ed. New York: Macmillan.

MORIMOTO, N. (1956). *Proc. Japan Acad.* **32**, 750–752.

MORIMOTO, N. & GÜVEN, N. (1970). *Amer. Min.*, **55**, 1195–1209.

MORIMOTO, N. & TOKONAMI, M. (1969). *Amer. Min.* **54**, 725–740.

NYE, J. F. (1957). *Physical Properties of Crystals.* Oxford Univ. Press.

PREWITT, C. T., PAPIKE, J. J. & ROSS, M. (1970). *Earth Planet. Sci. Lett.* **8**, 448.

TAKEDA, H. (1971). *Earth Planet. Sci. Lett.* **15**, 65–71.

Acta Cryst. (1975). A**31**, 130

Direct Structure Determination of Asymmetric Membrane Systems from X-ray Diffraction*

BY GLEN I. KING

Cardiovascular Research Institute, University of California at San Francisco, California 94143, *U.S.A.*

(*Received* 22 *April* 1974; *accepted* 11 *September* 1974)

A theoretical analysis of X-ray diffraction from asymmetric planar systems is given. Phase information is obtained from the continuous intensity function from such a system. Although a unique phase function cannot be determined, it is possible to derive the relatively small number of phase solutions which are consistent with the observed diffraction.

The structure of biological membranes is a subject of considerable current interest. X-ray diffraction studies have had a dominant role and have yielded much valuable information on this important topic. One fact about membrane ultrastructure which is slowly becoming evident is that most natural biological membranes (in contrast to artificial model lipid bilayer systems) are asymmetric. This asymmetry appears to be predominantly due to the protein component of the membrane (which is not to rule out the possibility of an asymmetric distribution of lipids in the membrane). Hence, the functional properties of the membrane are determined, in large part, from this property. Fortunately, many of the naturally occurring asymmetric membrane systems consist of repeating units of membrane pairs which have a center of symmetry. This permits the rather well developed theory of diffraction by centrosymmetric structures to be utilized in structure determination. However, there are many other membrane systems of interest where the former theory is not applicable (*e.g.*, dispersions of membrane vesicles and sheets). The present paper is concerned with the analysis of these asymmetric systems.

The difficulty in analyzing diffraction data from asymmetric structures (as well as symmetric ones) lies in the well-known phase problem of X-ray diffraction theory. There are indirect methods of obtaining this phase information (*e.g.* isomorphous replacement), but they have not been very useful for membranes. There has been much work in the past few years on direct methods of phase determination. These studies have shown that the X-ray diffraction intensity data contain some of the phase information necessary for a structural determination. Crucial to these studies has been the realization that the rather simple mathematical properties of positivity and boundedness of the electron density distribution (e.d.d.) place a severe restriction on its Fourier transform. In particular, the property

* This work was supported by NHLI Grant HL 06285.